

Abstract

The degree of non-linearity in DMS-cloud-climate interactions is assessed using the ECHAM5-HAMMOZ model by taking into account end-to-end aerosol chemistry-cloud microphysics link. The evaluation is made over the Southern oceans in austral summer, a region of minimal anthropogenic influence. In this study, we compare the DMS-derived changes in the aerosol and cloud microphysical properties between a baseline simulation with the ocean DMS emissions from a prescribed climatology, and a scenario where the DMS emissions are doubled. Our results show that doubling the DMS emissions in the current climate results in a non-linear response in atmospheric DMS burden and subsequently, in SO_2 and H_2SO_4 burdens due to inadequate OH oxidation. The aerosol optical depth increases by only $\sim 20\%$ in the 30°S – 75°S belt in the SH summer months. This increases the vertically integrated cloud droplet number concentrations (CDNC) by 25%. Since the vertically integrated liquid water vapor is constant in our model simulations, an increase in CDNC leads to a reduction in cloud droplet radius of 3.4% over the Southern oceans in summer. The equivalent increase in cloud liquid water path is 10.7%. The above changes in cloud microphysical properties result in a change in global annual mean radiative forcing at the TOA of -1.4 W m^{-2} . The results suggest that the DMS-cloud microphysics link is highly non-linear. This has implications for future studies investigating the DMS-cloud climate feedbacks in a warming world and for studies evaluating geoengineering options to counteract warming by modulating low level marine clouds.

1 Introduction

Aerosols can influence the radiative balance of the Earth both directly and indirectly. They can absorb and scatter the incoming solar and outgoing infrared radiation and impart a direct radiative forcing to the climate system. Aerosols can also act as cloud condensation nuclei, alter the microphysical properties of clouds and impose an indirect

Non-linearity in DMS-cloud-climate interactions

M. A. Thomas et al.

Title Page

Abstract

Introduction

Conclusions

References

Tables

Figures

⏪

⏩

◀

▶

Back

Close

Full Screen / Esc

Printer-friendly Version

Interactive Discussion



**Non-linearity in
DMS-cloud-climate
interactions**M. A. Thomas et al.

[Title Page](#)[Abstract](#)[Introduction](#)[Conclusions](#)[References](#)[Tables](#)[Figures](#)[⏪](#)[⏩](#)[◀](#)[▶](#)[Back](#)[Close](#)[Full Screen / Esc](#)[Printer-friendly Version](#)[Interactive Discussion](#)

radiative forcing to the climate system (Carslaw et al., 2010; Lohmann and Feichter, 2005 and references therein). The first indirect aerosol effect concerns the change in cloud albedo due to an increase in cloud condensation nuclei (CCN) concentration. The increased CCN load leads to an increased number of smaller cloud droplets under constant liquid water content (Twomey, 1974, 1977). Smaller cloud droplets reduce the coalescence efficiency resulting in an increase in the lifetime of clouds, which results in the second indirect aerosol effect, also known as the cloud lifetime effect (Albrecht, 1989).

Aerosol indirect effects are considered to be among the largest source of uncertainties in radiative forcing estimates derived from global chemistry-climate models (Solomon et al., 2007). Reviews of model estimates of indirect aerosol effects (IAE) are given in Lohmann and Feichter (2005); Quaas et al. (2009); Carslaw et al. (2010). These studies indicate that both the first and second indirect aerosol effects tend to cool the Earth-atmosphere system, with TOA (top of the atmosphere) radiative forcing estimates ranging from -0.5 to -1.9 W m^{-2} for the first indirect aerosol effect and from -0.3 to -1.4 W m^{-2} for the second indirect aerosol effect. This range in the TOA radiative forcing results from model specific variations in the representation of aerosol species, aerosol microphysics and aerosol-cloud interactions. When these models are constrained by satellite data, the forcing is estimated as $-0.7 \pm 0.4 \text{ W m}^{-2}$ (Quaas et al., 2009).

In order to estimate indirect aerosol radiative forcing more accurately, it is important to evaluate and understand non-linearities in the aerosol-cloud-climate system. This information will also help towards evaluation of recently proposed geoengineering options involving alteration of low level cloud systems (for example, the recent studies by Boyd, 2008; Jones et al., 2009; Korhonen et al., 2010; Wingenter et al., 2007; Woodhouse et al., 2008).

Some earlier studies have noted potential non-linearity in aerosol-CDNC formation pathways. For example, Pandis et al. (1994) and Russell et al. (1994) show that under low DMS emissions, the DMS-CCN link is non-linear due to heterogeneous reactions

on sea salt; the link is likely to be linear in pristine marine conditions when DMS fluxes are higher ($>2.5 \mu\text{mol m}^{-2} \text{d}^{-1}$). More recently, in the context of geoengineering, Woodhouse et al. (2008) have demonstrated that the conversion of DMS to aerosol and CCN does not scale linearly and can not be represented by a simple production efficiency.

5 By increasing the DMS sea water concentrations five fold, a 1.4% increase in CCN was simulated over the Southern oceans, compared to a 10% increase estimated by Wingenter et al. (2007). Using a fully coupled atmosphere-ocean climate model, Jones et al. (2009) and Rasch et al. (2009) examined the impact of directly increasing CDNC in the low level marine stratocumulus cloud regions by setting the CDNC in the models
10 to 375 cm^{-3} and 1000 cm^{-3} respectively, thereby suggesting methods that may help to override the effects of global warming, though the response was not uniform globally. Instead of imposing an increase of CDNC, Korhonen et al. (2010) used a global aerosol transport model to quantify the change in droplet number concentrations resulting from an increase in sea salt emissions as prescribed by Salter et al. (2008); they
15 showed that the pathway from the emissions to CDNC formation was non linear because of the dilution and removal of particles from the atmosphere, and also because the injection of a large number of accumulation mode particles suppressed cloud supersaturation. The regional median CDNC in their study in the seeded regions range from $246\text{--}314 \text{ cm}^{-3}$ which is much lower than the CDNC values assumed by Latham
20 et al. (2008) and Jones et al. (2009).

While deriving motivation from the above results, the present study extends them by using a global aerosol-chemistry-cloud microphysics-climate model (ECHAM5-HAMMOZ) that accounts directly for the process based linkages between DMS emissions, aerosol formation, and cloud microphysics. We will evaluate the degree of non-linearity in the downstream formation of sulphate, in aerosol optical depth, in cloud
25 microphysical properties such as CDNC, CD effective radii, liquid water path, and in TOA radiative forcing.

Non-linearity in DMS-cloud-climate interactions

M. A. Thomas et al.

Title Page

Abstract

Introduction

Conclusions

References

Tables

Figures

◀

▶

◀

▶

Back

Close

Full Screen / Esc

Printer-friendly Version

Interactive Discussion



2 Model, experimental set up and methodology

Details of the configuration of our DMS-sulfate aerosol simulations using ECHAM5-HAMMOZ were presented in Thomas et al. (2010). ECHAM5-HAMMOZ consists of the general circulation model, ECHAM5 (Roeckner and co authors, 2003), aerosol module, HAM (Stier et al., 2005) and a detailed tropospheric chemistry module, MOZ (Horowitz et al., 2003). Details on the validation of aerosol and cloud parameters are given in the literature (Pozzoli et al., 2008a,b; Rast et al., 2008; Thomas et al., 2010). In the model, aerosol optical depth is obtained from a look up table of offline Mie calculations given the complex volume weighted mean refractive index of each aerosol mode taking into consideration all the aerosol components and aerosol water and the median radius. Aerosol-cloud interactions are parameterized using the cloud microphysics scheme described in Lohmann et al. (2007). A prognostic equation is used to describe the relationship between aerosol number concentration and cloud droplet nucleation. This equation accounts for the microphysical processes such as nucleation, autoconversion, self-collection, accretion by rain and snow, freezing and evaporation of cloud droplets. The autoconversion rate of cloud droplets to form raindrops is important for the cloud lifetime effect and is parameterized based on cloud liquid water mass mixing ratio and the cloud droplet number concentration (Khairoutdinov and Kogan, 2000). The nucleation rate of cloud droplets is based on the total number of aerosols, the updraft velocity and a factor, which takes the aerosol composition and size spectrum into account (Chuang and Penner, 1995). The cloud fraction is predicted based on the parameterization scheme by Tompkins (2002). The effective radius for cloud droplets is obtained from the mean volume radius and a simple parameterization of the dispersion effect that depends on the cloud droplet number concentration (Peng and Lohmann, 2003).

Simulations are performed with T42L31 ($\sim 2.8 \times 2.8^\circ$ and 31 levels from surface to 10 hPa) resolution by nudging the model with the ECMWF ERA-40 meteorological fields for the year 1999/2000. In Thomas et al. (2010), two simulations were carried

Non-linearity in DMS-cloud-climate interactions

M. A. Thomas et al.

Title Page

Abstract

Introduction

Conclusions

References

Tables

Figures



Back

Close

Full Screen / Esc

Printer-friendly Version

Interactive Discussion



Non-linearity in DMS-cloud-climate interactions

M. A. Thomas et al.

Title Page

Abstract

Introduction

Conclusions

References

Tables

Figures

◀

▶

◀

▶

Back

Close

Full Screen / Esc

Printer-friendly Version

Interactive Discussion



out: (1) “CTRL” simulation for which the ocean DMS sea water concentrations were prescribed from the Kettle and Andreae (2000) climatology and (2) a “wo_ODMS” simulation with no ocean DMS emissions. In the present study, we perform, in addition, a 12-month simulation (December 1999–November 2000) in which the ocean DMS sea water concentrations is doubled (referred to as “2X_ODMS”, hereafter in the text). Other emissions include anthropogenic and wildfire SO_2 , black carbon and organic carbon from the background aerosol concentrations, and are held fixed in our simulations in addition to the interactively computed sea salt and dust emissions. Over the Southern oceans, in addition to DMS emissions, the dominant aerosol species are wind generated sea spray particles which in the model, is parameterized following Monahan et al. (1986) scheme (for particles in the range 0.1 to 10 μm) and Smith and Harrison (1998) scheme (for the coarse particle range). The DMS-sea salt interactions in the model are described in detail in Thomas et al. (2010). Our analysis mainly focuses on the Southern ocean region, where anthropogenic influence is minimal and during SH summer months when low level clouds are prevalent.

We evaluate the impact of changes in DMS emissions on cloud microphysical properties and radiative forcing using the following diagnostics.

$$\text{DIAG1} = [(\text{CTRL} - \text{wo_ODMS}) / \text{wo_ODMS}] \times 100\%$$

$$\text{DIAG2} = [(2\text{X_ODMS} - \text{wo_ODMS}) / \text{wo_ODMS}] \times 100\%$$

$$\text{DIAG3} = [(2\text{X_ODMS} - \text{CTRL}) / \text{CTRL}] \times 100\%$$

The diagnostics, DIAG1 and DIAG2 give the mean percentage change in the present day DMS emissions and in a doubled DMS scenario relative to a scenario with no DMS emissions. The comparison of DIAG1 and DIAG2 would give insight into the non-linearity of the system. The DIAG3 measure is the mean percentage change in the aerosol parameters and cloud microphysics when the ocean DMS is doubled with respect to the present day DMS emissions.

3 Results and discussion

3.1 Non-linearity in DMS-aerosol chemistry link

The seasonal cycle and magnitude of the ocean DMS flux to the atmosphere in a doubled DMS sea water concentrations case and in the CTRL simulation averaged over the Southern oceans and globally is shown in Fig. 1. The seasonality in the fluxes follow that of the CTRL simulation, except that the magnitude is doubled. In the 2X_ODMS case, the mean DMS emissions in austral summer is about $8.17 \times 10^{-12} \text{ Kg(S) m}^{-2} \text{ s}^{-1}$ when averaged over the $30^\circ \text{ S} - 75^\circ \text{ S}$ latitudinal belt compared to a value of $4.08 \times 10^{-12} \text{ Kg(S) m}^{-2} \text{ s}^{-1}$ in the CTRL simulation. The mean winter fluxes are respectively around $1.36 \times 10^{-12} \text{ Kg(S) m}^{-2} \text{ s}^{-1}$ and $0.7 \times 10^{-12} \text{ Kg(S) m}^{-2} \text{ s}^{-1}$ in 2X_ODMS simulation and CTRL simulations. Globally, the austral summer mean (annual mean) DMS flux to the atmosphere ranges from $1.95 \times 10^{-12} \text{ Kg(S) m}^{-2} \text{ s}^{-1}$ ($1.45 \times 10^{-12} \text{ Kg(S) m}^{-2} \text{ s}^{-1}$) in the CTRL simulation to $3.91 \times 10^{-12} \text{ Kg(S) m}^{-2} \text{ s}^{-1}$ ($2.90 \times 10^{-12} \text{ Kg(S) m}^{-2} \text{ s}^{-1}$) in the 2X_ODMS simulation, indicating a linear response. However, the atmospheric DMS burden for the austral summer mean months averaged over the southern latitude belt is 0.034 Tg(S) in the CTRL run (the global annual mean atmospheric DMS burden in CTRL is 0.050 Tg(S)) and 0.106 Tg(S) in the 2X_ODMS run. The DMS burden is tripled when the ocean DMS emissions are doubled. This means that DMS is not converted to SO_2 by OH oxidation in 2X_ODMS at same rate as in the CTRL. OH concentration is not sufficient to oxidize all the DMS when the emissions are doubled, so DMS accumulates, resulting in a three fold increase in the DMS burden.

The diagnostics for SO_2 and H_2SO_4 column burdens, vertically integrated activated particle number concentration and AOD are presented in Table 1 during the mean austral summer months over $30^\circ \text{ S} - 75^\circ \text{ S}$ mean latitude belt (The absolute numbers for the above mentioned parameters in wo_ODMS, CTRL and 2X_ODMS simulations are given in Table 1 in the Supplement). Relative to the wo_ODMS emissions, both SO_2 and H_2SO_4 burden increases by approximately 118% in the CTRL simulation.

Non-linearity in DMS-cloud-climate interactions

M. A. Thomas et al.

Title Page

Abstract

Introduction

Conclusions

References

Tables

Figures

◀

▶

◀

▶

Back

Close

Full Screen / Esc

Printer-friendly Version

Interactive Discussion



This points out to the efficient conversion of SO_2 to H_2SO_4 or in other words, there is sufficient OH to facilitate the conversion of the SO_2 to H_2SO_4 . However, the percentage increase is 294.5 % and 180.6 % respectively for SO_2 and H_2SO_4 column burdens in the 2X_ODMS simulation. A non-linear response is evident in both SO_2 and H_2SO_4 burdens. In DIAG3, the increase in burdens of SO_2 and H_2SO_4 concentrations are 80.9 % and only 28.2 % respectively in the 2X_ODMS simulation compared to the CTRL simulation. The relatively small percentage increase in all the diagnostics in the H_2SO_4 burden compared to the SO_2 burden and the non-linearity can be explained as follows: the atmospheric DMS is converted to SO_2 by the reactions with OH and NO_3 (Pozzoli et al., 2008a; Stier et al., 2005; Feichter et al., 1996) which is further oxidized to H_2SO_4 . SO_2 is at the equilibrium between the gas- and aqueous- phases, the total dissolved SO_2 depends on its partial pressure and the Henry's law constant, which increases by almost seven orders of magnitude as the pH increases from 1 to 8. In the gas-phase, the reaction with the OH radical is dominant, produces sulfuric acid (H_2SO_4), which rapidly gets converted to sulfate aerosol by nucleation and condensation. The SO_2 dissolved in the aqueous-phase produces sulfate aerosol when oxidized by O_3 and H_2O_2 (SO_2 in-cloud oxidation). In our simulations the sulfate production in the liquid phase is very much linear (not shown here) with doubling ocean DMS emissions. Also, the deposition (dry,wet and sedimentation) ratio, 2X_ODMS/CTRL is lower than 2. This means that there is a lower production of SO_4 from gas phase oxidation. The higher percentage increase in SO_2 concentrations compared to the H_2SO_4 is because of the lower OH oxidation taking place and hence, SO_2 accumulates, thereby exhibiting a non-linear response in SO_2 and H_2SO_4 burdens to the doubling of ocean DMS.

The vertically integrated number of activated particles over the southern oceans in austral summer increase by 116.7 % in CTRL simulation and 179.2 % in 2X_ODMS simulation relative to the wo_ODMS. It can be seen that the rate of increase is not doubled and does not scale up with the doubling of DMS emissions, hence the pathway is non-linear. The number of activated particles is calculated based on the supersaturation and updraft velocity that depends non-linearly on the total aerosol number and their

Non-linearity in DMS-cloud-climate interactions

M. A. Thomas et al.

Title Page

Abstract

Introduction

Conclusions

References

Tables

Figures

◀

▶

◀

▶

Back

Close

Full Screen / Esc

Printer-friendly Version

Interactive Discussion



size distribution and chemical composition. The number of activated particles increase by only 28.9% with the doubling of ocean DMS compared to the CTRL simulation. This is due to the saturation effect whereby enhanced aerosol concentrations diminish the supersaturation hindering activation of aerosol particles (Boucher and Lohmann, 1994).

The resulting zonal mean DMS derived aerosol optical depth (AOD) at 0.55 μm for the latitude belt 30° S–75° S is 0.167 in the CTRL simulation and 0.2013 in the 2X_ODMS simulation for the SH summer months. The percentage increase in AOD in the 2X_ODMS simulation with respect to the CTRL simulation and also, for DIAG1 and DIAG2 diagnostics are presented in Table 1. The aerosol optical depth is indirectly coupled to aerosol numbers and mass through size distribution, composition and mixing state. The percentage increases in AOD in DIAG1 and DIAG2 are 23.1% and 50.3%. Relative to the no DMS emission scenario, the AOD is mostly doubled when the emissions in the CTRL simulation are doubled, indicating a linear behaviour. However, DIAG3 shows that with a doubling of model ocean DMS, the model AOD increases by ~20% over the SH summer months in the 30° S–75° S belt relative to the CTRL simulation. Here, a non-linear response is seen when the emissions are doubled in the CTRL scenario.

The following subsections describe in detail the changes in the modelled cloud microphysical properties (such as CDNC burden, CD effective radii and cloud liquid water path) for a doubling of the ocean DMS flux. We also discuss the variation in the top of the atmosphere all sky radiative forcing. The changes are evaluated based on the diagnostics given in Sect. 2.

Non-linearity in DMS-cloud-climate interactions

M. A. Thomas et al.

Title Page

Abstract

Introduction

Conclusions

References

Tables

Figures



Back

Close

Full Screen / Esc

Printer-friendly Version

Interactive Discussion



3.2 Non-linearity in cloud microphysical link

3.2.1 CDNC burden

The zonally averaged CDNC burden averaged over the Southern oceans [30° S–75° S] is presented in Fig. 2 for the CTRL simulation (black line), wo_ODMS simulation (red line) and for the 2X_ODMS simulation (green line). An increase in CDNC burden in both CTRL and 2X_ODMS simulations compared to the wo_ODMS simulation is clearly evident. This increase is more pronounced in the austral summer months, associated with the intense biological activity during this period of the year and a minimum in the austral winter months. Also, it has to be noted that the CDNC burden increases with the doubling of the DMS emissions. Summarized in Table 2 for the SH summer months, averaged over the 30° S–75° S latitude belt, the CDNC burden is increased by 165 % for the 2X_ODMS and 110 % for the CTRL compared to the simulation with no DMS emissions (DIAG1 and DIAG2 respectively). This indicates that the processes governing the CDNC formation are non-linear, as the CDNC burden does not scale with the DMS emissions. The vertically integrated atmospheric liquid water remains constant in all these simulations which is one of the reasons why while the DMS emissions increase two fold, the droplet number concentrations increase by only 25 % over the 30° S–75° S latitude belt during SH summer (refer DIAG3 in Table 2) due to the saturation effect explained in the previous section and is in sync with the change in the number of activated particles. Boucher and Lohmann (1994) used an empirical relationship in their indirect effect parameterization between CDNC and sulfate mass and showed that an increase in CDNC with increasing aerosol load can take place only in relatively clean air. Globally, the CDNC burden increases by only 13.2 % (13.1 %) when the DMS emissions are doubled when averaged over DJF months (averaged annually).

Non-linearity in DMS-cloud-climate interactions

M. A. Thomas et al.

Title Page

Abstract

Introduction

Conclusions

References

Tables

Figures

◀

▶

◀

▶

Back

Close

Full Screen / Esc

Printer-friendly Version

Interactive Discussion



3.2.2 CD effective radii

In Fig. 3 we present variations in the cloud top cloud droplet effective radii in the CTRL (black), wo_ODMS (red) and 2X_ODMS (green) simulations. The droplet size reaches a maximum of $12.2\ \mu\text{m}$ in the wo_ODMS case during the austral summer months. In both the CTRL and 2X_ODMS simulations, the droplet size is smaller (between $10.5\ \mu\text{m}$ and $11.5\ \mu\text{m}$) compared to the droplet size with no ocean DMS emissions. Also, it is evident that the droplet radius is even smaller when the DMS is doubled compared to the DMS in the CTRL simulation. The percentage differences of the simulated droplet radii presented in Table 3 in the CTRL (DIAG1) and 2X_ODMS (DIAG2) shows that the droplet radius is smaller by about 6% and 9% respectively compared to the droplet size in the wo_ODMS simulation when averaged over 30°S – 75°S latitude belt in DJF, a clear signature of the first indirect aerosol effect. The cloud droplet radius is primarily determined by liquid water content in the cloud and CDNC, which depends on the number of aerosol particles. There are more activated particles in the 2X_ODMS simulation competing for the same amount of available atmospheric water (with only 0.11% increase in 2X_ODMS compared to CTRL), thereby, resulting in a reduction in the droplet size. Here, we can see that the decrease in droplet size with a two fold increment in DMS emissions is non-linear. The DIAG3 gives the variation in the droplet radii in the 2X_ODMS compared to the DMS emissions in the CTRL simulation. The mean decrease is 2.9% when the DMS emissions are doubled.

3.2.3 Cloud liquid water path

The second IAE or the cloud lifetime effect is manifested as an increase in cloud liquid water path and hence, cloud cover. A decrease in cloud droplet effective radius due to an increase in aerosol amount leads to the decreased coalescence efficiency of cloud droplets. This further results in precipitation suppression and increase in cloud lifetime. The vertically integrated cloud liquid water in the three simulations carried out here are

Non-linearity in DMS-cloud-climate interactions

M. A. Thomas et al.

Title Page

Abstract

Introduction

Conclusions

References

Tables

Figures



Back

Close

Full Screen / Esc

Printer-friendly Version

Interactive Discussion



presented in Fig. 4. Here, it can be seen that there is an increase in cloud liquid water path when ocean DMS is included (black and green lines) in the simulations compared to the no DMS case (red line). This is because, the rate at which cloud droplets form rain drops is inversely proportional to CDNC, which means that an increase in aerosol concentrations and hence, CDNC delays the precipitation rate leading to increased liquid water path (Lohmann and Feichter, 1997). The seasonality observed in the CTRL and the 2X_ODMS simulations also follows the ocean DMS cycle with a maximum over the austral summer months and a minimum over the austral winter months. The cloud liquid water path increases with the doubling of ocean DMS over the 30° S–75° S latitude belt when compared to the CTRL scenario run.

Table 4 gives the percentage changes in the vertically integrated cloud liquid water over the Southern oceans in SH summer. An increase of approximately 44 % in the CTRL and 61 % in the 2X_ODMS simulation with respect to the wo_ODMS simulation is simulated over the SH summer months when averaged south of 30S. Maximum increase in the cloud liquid water path is seen in the northern most band in the 30° S–75° S latitude band, with an average increase of 11.7 % over the Southern oceans, when the DMS emissions are doubled with respect to the DMS emissions in the CTRL simulation. Globally, an annual mean increase of 7.5 % is estimated when the DMS emissions are doubled compared to the CTRL simulation which corresponds to a 0.35 % increase in the total cloud cover (not shown).

3.3 Aerosol radiative forcing at the TOA

The TOA all sky radiative forcing is evaluated as the difference between the perturbed (CTRL and 2X_ODMS simulations) and the unperturbed (wo_ODMS) radiative fluxes (Thomas et al., 2010). The global annual mean DMS induced aerosol radiative forcing at the TOA is estimated as -2.03 W m^{-2} in the CTRL simulation and -3.42 W m^{-2} in the doubling DMS simulation. This means that under near constant atmospheric water vapor, a doubling of the DMS emissions can result in an additional cooling of

Non-linearity in DMS-cloud-climate interactions

M. A. Thomas et al.

Title Page

Abstract

Introduction

Conclusions

References

Tables

Figures



Back

Close

Full Screen / Esc

Printer-friendly Version

Interactive Discussion



-1.4 W m^{-2} compared to the ocean DMS emissions in the CTRL simulation. Note that the current net global anthropogenic radiative forcing is $\sim 1.6 \text{ W m}^{-2}$ compared to pre-industrial values (Solomon et al., 2007).

The TOA radiative forcing over the Southern oceans during the SH austral months are presented in Table 5 in the CTRL (given in brackets) and in the 2X_ODMS simulations. The values have a maximum of -24 W m^{-2} and a minimum of -6 W m^{-2} over the Southern oceans during SH summer for the 2X_ODMS case. In the CTRL scenario case, the radiative forcing at the TOA range between -14 W m^{-2} and -5 W m^{-2} . The largest changes (5 W m^{-2}) in the TOA radiative forcing for the 2X_ODMS case in comparison to the CTRL occur in the 30° S – 60° S latitude band. However, the variation in the TOA radiative forcing pertaining to a doubling of DMS is relatively small (maximum decrease is -2.3 W m^{-2}) in the Southern most belt in the SH.

4 Summary and conclusions

An assessment of the degree of non-linearity in DMS-cloud-climate interactions is crucial as it has implications for our understanding of these links in future climate as well as evaluation of geoengineering studies that propose to modulate low-level marine water clouds. The global model ECHAM5-HAMMOZ enables us to investigate such non-linearity in different processes by taking into account the linked chemistry, aerosol and cloud microphysical processes. For this, we compared the DMS derived changes in the cloud microphysical properties between a control simulation and one in which DMS emissions were doubled. Simulations are carried out in the T42L31 resolution by forcing the model with ERA-40 meteorological fields for 13 months from Dec 1999. In these simulations the vertically integrated atmospheric water vapor is a constant. In the control simulation, the ocean DMS concentration is prescribed from the Kettle and Andreae (2000) database.

The main findings of this paper are summarized below. The DMS flux to the atmosphere is $8.34 \times 10^{-12} \text{ Kg(S) m}^{-2} \text{ s}^{-1}$ in the CTRL simulation. With the doubling of the

Non-linearity in DMS-cloud-climate interactions

M. A. Thomas et al.

Title Page

Abstract

Introduction

Conclusions

References

Tables

Figures

◀

▶

◀

▶

Back

Close

Full Screen / Esc

Printer-friendly Version

Interactive Discussion



DMS emissions, we increase the H_2SO_4 burden by only 28 %, SO_2 burden by 81 % and AOD by ~ 20 % over the SH summer months in the 30°S – 75°S belt. This resulted in an increase in the vertically integrated CDNCs by 25 %. Since the vertically integrated atmospheric liquid water vapor is a constant, an increase in CDNCs leads to a reduction in cloud droplet radius. We simulate a decrease by 3.4 % in the droplet radius over the Southern oceans in DJF. The equivalent increase in cloud liquid water path is 10.7 %. These percentage deviations do not change substantially when averaged over the globe, as the largest changes in the DMS aerosol-cloud-climate interactions are observed over the Southern oceans which is a region of maximum DMS emissions during the SH summer. The aforementioned changes in cloud microphysical properties results in a global annual mean cooling at the TOA of -3.42 W m^{-2} ; an additional cooling of -1.4 W m^{-2} when the DMS emissions to the atmosphere are doubled. The results from our study implies that the aerosol chemistry-cloud microphysics link is highly non-linear. Finally, we would like to mention that the discussions on geoengineering methodologies that propose modulations of low-level marine water clouds are centered mainly on two aerosol proposals: one where the injection of sea salt aerosols to counteract warming is envisaged, and the other, where iron fertilization in oceans is estimated to stimulate DMS-cloud climate interactions. The present study would provide useful insights in evaluating the latter proposal.

Supplementary material related to this article is available online at:
[http://www.atmos-chem-phys-discuss.net/11/15227/2011/
acpd-11-15227-2011-supplement.pdf](http://www.atmos-chem-phys-discuss.net/11/15227/2011/acpd-11-15227-2011-supplement.pdf).

Non-linearity in DMS-cloud-climate interactions

M. A. Thomas et al.

Title Page

Abstract

Introduction

Conclusions

References

Tables

Figures

⏪

⏩

◀

▶

Back

Close

Full Screen / Esc

Printer-friendly Version

Interactive Discussion



Acknowledgements. This work was supported and funded by the QUEST-feedbacks project under the UK Natural Environment Research Council (NERC) QUEST programme.

References

- Albrecht, B.: Aerosols, cloud microphysics and fractional cloudiness, *Science*, 245, 1227–1230, 1989. 15229
- Boucher, O. and Lohmann, U.: The sulfate-CCN-cloud albedo effect, *Tellus B*, 47, 281–300, 1994. 15235, 15236
- Boyd, P. W.: Ranking geo-engineering schemes, *Nat. Geosci.*, 1, 722–724, 2008. 15229
- Carslaw, K. S., Boucher, O., Spracklen, D. V., Mann, G. W., Rae, J. G. L., Woodward, S., and Kulmala, M.: A review of natural aerosol interactions and feedbacks within the Earth system, *Atmos. Chem. Phys.*, 10, 1701–1737, doi:10.5194/acp-10-1701-2010, 2010. 15229
- Chuang, C. C. and Penner, J. E.: Effects of anthropogenic sulfate on cloud drop nucleation and optical properties, *Tellus B*, 47, 566–577, 1995. 15231
- Feichter, J., Kjellstrom, E., Rodhe, H., Dentener, F., Lelieveld, J., and Roelofs, G.: Simulation of the tropospheric sulfur cycle in a global climate model, *Atmos. Environ.*, 30, 1693–1707, 1996. 15234
- Horowitz, L. W., Walters, S., Mauzerall, D. L., Emmons, L. K., Rasch, P. J., Granier, C., Tie, X., Lamarque, J., Schultz, M. G., Tyndall, G. S., Orlando, J. J., and Brasseur, G. P.: A global simulation of tropospheric ozone and related tracers: Description and evaluation of MOZART, version 2, *J. Geophys. Res.*, 108(D24), 4784, doi:10.1029/2002JD002853, 2003. 15231
- Jones, A., Haywood, J., and Boucher, O.: Climate impacts of geoengineering marine stratocumulus clouds, *J. Geophys. Res.*, 114, D10106, doi:10.1029/2008JD011450, 2009. 15229, 15230
- Kettle, A. and Andreae, M.: Flux of dimethylsulfide from the oceans: A comparison of updated data sets and flux models, *J. Geophys. Res.*, 105, 26793–26808, 2000. 15232, 15239
- Khairoutdinov, M. and Kogan, Y.: A new cloud physics parameterization in a large-eddy simulation model of marine stratocumulus, *Mon. Weather Rev.*, 128, 229–243, 2000. 15231
- Korhonen, H., Carslaw, K. S., and Romakkaniemi, S.: Enhancement of marine cloud albedo via controlled sea spray injections: a global model study of the influence of emission rates,

Non-linearity in DMS-cloud-climate interactions

M. A. Thomas et al.

Title Page

Abstract

Introduction

Conclusions

References

Tables

Figures

◀

▶

◀

▶

Back

Close

Full Screen / Esc

Printer-friendly Version

Interactive Discussion



microphysics and transport, *Atmos. Chem. Phys.*, 10, 4133–4143, doi:10.5194/acp-10-4133-2010, 2010. 15229, 15230

Latham, J., Rasch, P., Chen, C.-C., Kettles, L., Gadian, A., Gettelman, A., Morrison, H., Bower, K., and Choulaton, T.: Global temperature stabilization via controlled albedo enhancement of low-level maritime clouds, *Philos. T. R. Soc. A*, 366(1882), 3969–3987, 2008. 15230

Lohmann, U. and Feichter, J.: Impact of sulfate aerosols on albedo and lifetime of clouds: A sensitivity study with the ECHAM4 GCM, *J. Geophys. Res.*, 102(D12), 13685–13700, 1997. 15238

Lohmann, U. and Feichter, J.: Global indirect aerosol effects: a review, *Atmos. Chem. Phys.*, 5, 715–737, doi:10.5194/acp-5-715-2005, 2005. 15229

Lohmann, U., Stier, P., Hoose, C., Ferrachat, S., Kloster, S., Roeckner, E., and Zhang, J.: Cloud microphysics and aerosol indirect effects in the global climate model ECHAM5-HAM, *Atmos. Chem. Phys.*, 7, 3425–3446, doi:10.5194/acp-7-3425-2007, 2007. 15231

Monahan, E., Spiel, D., and Davidson, K.: Oceanic whitecaps and their role, in: air-sea exchange, chapter: A model of marine aerosols generation via whitecaps and wave disruption, D. Reidel, Norwell, Massachusetts, 252 ed., 167–174, 1986. 15232

Pandis, S. N., Russell, L. M., and Seinfeld, J. H.: The relationship between DMS flux and CCN concentrations in remote marine regions, *J. Geophys. Res.*, 99, 16945–16957, 1994. 15229

Peng, Y. and Lohmann, U.: Sensitivity study of the spectral dispersion of the cloud droplet size distribution on the indirect aerosol effect, *Geophys. Res. Lett.*, 30(10), 1507, doi:10.1029/2003GL017192, 2003. 15231

Pozzoli, L., Bey, I., Rast, J. S., Schultz, M. G., Stier, P., and Feichter, J.: Trace gas and aerosol interactions in the fully coupled model of aerosol-chemistry-climate ECHAM5-HAMMOZ: 1. Model description and insights from the spring 2001 TRACE-P experiment, *J. Geophys. Res.*, 113, D07308, doi:10.1029/2007JD009007, 2008a. 15231, 15234

Pozzoli, L., Bey, I., Rast, J. S., Schultz, M. G., Stier, P., and Feichter, J.: Trace gas and aerosol interactions in the fully coupled model of aerosol-chemistry-climate ECHAM5-HAMMOZ: 2. Impact of heterogeneous chemistry on the global aerosol distributions, *J. Geophys. Res.*, 113, D07309, doi:10.1029/2007JD009008, 2008b. 15231

Quaas, J., Ming, Y., Menon, S., Takemura, T., Wang, M., Penner, J. E., Gettelman, A., Lohmann, U., Bellouin, N., Boucher, O., Sayer, A. M., Thomas, G. E., McComiskey, A., Feingold, G., Hoose, C., Kristjánsson, J. E., Liu, X., Balkanski, Y., Donner, L. J., Ginoux, P. A., Stier, P., Grandey, B., Feichter, J., Sednev, I., Bauer, S. E., Koch, D., Grainger, R. G., Kirkevåg, A.,

ACPD

11, 15227–15253, 2011

Non-linearity in DMS-cloud-climate interactions

M. A. Thomas et al.

Title Page

Abstract

Introduction

Conclusions

References

Tables

Figures

◀

▶

◀

▶

Back

Close

Full Screen / Esc

Printer-friendly Version

Interactive Discussion



Non-linearity in DMS-cloud-climate interactions

M. A. Thomas et al.

Title Page

Abstract

Introduction

Conclusions

References

Tables

Figures

◀

▶

◀

▶

Back

Close

Full Screen / Esc

Printer-friendly Version

Interactive Discussion



Iversen, T., Seland, Ø., Easter, R., Ghan, S. J., Rasch, P. J., Morrison, H., Lamarque, J.-F., Iacono, M. J., Kinne, S., and Schulz, M.: Aerosol indirect effects - general circulation model intercomparison and evaluation with satellite data, *Atmos. Chem. Phys.*, 9, 8697–8717, doi:10.5194/acp-9-8697-2009, 2009. 15229

5 Rast, S., Schultz, M. G., Bey, I., van Noije, T., Aghedo, A. M., Brasseur, G. P., Diehl, T., Esch, M., Ganzeveld, L., Kirchner, I., Kornblueh, L., Rhodin, A., Roeckner, E., Schmidt, H., Schroeder, S., Schulzweida, U., Stier, P., Thomas, K., and Walters, S.: Evaluation of the tropospheric chemistry general circulation model ECHAM5-MOZ and its application to the analysis of interannual variability in tropospheric ozone from 1960–2000, *J. Geophys. Res.*, submitted, 2008. 15231

10 Rasch, P. J., Latham, J., and Chen, C. C.: Geoengineering by cloud seeding: Influence on sea ice and climate system., *Environ. Res. Lett.*, 4, 8 pp., 2009. 15230

Roeckner, E., Baeuml, G., Bonaventura, L., Brokopf, R., Esch, M., Giorgetta, M., Hagemann, S., Kirchner, I., Kornblueh, L., Manzini, E., Rhodin, A., Schlese, U., Schulzweida, U., and Tompkins, A.: The atmospheric general circulation model ECHAM5. PART I: Model description., *MPI-Report*, 349, 127 pp., 2003. 15231

15 Russell, L. M., Pandis, S. N., and Seinfeld, J. H.: Aerosol production and growth in the marine boundary layer, *J. Geophys. Res.*, 99, 20989–21003, 1994. 15229

Salter, S., Sortino, G., and Latham, J.: Sea-going hardware for the cloud albedo method of reversing global warming., *Phil. Trans. R. Soc.*, A366, 3989–4006, 2008. 15230

20 Smith, M. and Harrison, N.: The sea spray generation function, *J. Aerosol Sci.*, 29, 189–190, 1998. 15232

Solomon, S., Qin, D., Manning, M., Chen, Z., Marquis, M., Averyt, K. M., and Tignor, H. M.: IPCC, 2007: Summary for Policymakers, in: *Climate Change 2007: The Physical Science Basis. Contribution of Working Group I to the Fourth Assessment Report of the Intergovernmental Panel on Climate Change*, Cambridge University Press, Cambridge, United Kingdom and New York, NY, USA, 2007. 15229, 15239

25 Stier, P., Feichter, J., Kinne, S., Kloster, S., Vignati, E., Wilson, J., Ganzeveld, L., Tegen, I., Werner, M., Balkanski, Y., Schulz, M., Boucher, O., Minikin, A., and Petzold, A.: The aerosol-climate model ECHAM5-HAM, *Atmos. Chem. Phys.*, 5, 1125–1156, doi:10.5194/acp-5-1125-2005, 2005. 15231, 15234

30 Thomas, M. A., Suntharalingam, P., Pozzoli, L., Rast, S., Devasthale, A., Kloster, S., Feichter, J., and Lenton, T. M.: Quantification of DMS aerosol-cloud-climate interactions using the

Non-linearity in DMS-cloud-climate interactions

M. A. Thomas et al.

Title Page

Abstract

Introduction

Conclusions

References

Tables

Figures

⏪

⏩

◀

▶

Back

Close

Full Screen / Esc

Printer-friendly Version

Interactive Discussion



ECHAM5-HAMMOZ model in a current climate scenario, *Atmos. Chem. Phys.*, 10, 7425–7438, doi:10.5194/acp-10-7425-2010, 2010. 15231, 15232, 15238

Tompkins, A. M.: A prognostic parameterization for the subgrid-scale variability of water vapor and clouds in large-scale models and its use to diagnose cloud cover, *J. Atmos. Sci.*, 59, 1917–1942, 2002. 15231

Twomey, S. A.: Pollution and the Planetary Albedo, *Atmos. Environ.*, 8, 1251–1256, 1974. 15229

Twomey, S. A.: The influence of pollution on the shortwave albedo of clouds, *J. Atmos. Sci.*, 34, 1149–1152, 1977. 15229

Wingenter, O. W., Elliot, S. M., and Blake, D. R.: New directions: Enhancing the natural sulphur cycle to slow global warming, *Atmos. Environ.*, 41, 7373–7375, 2007. 15229, 15230

Woodhouse, M. T., Mann, G. W., and Carslaw, K. S.: New Directions: The impact of oceanic iron fertilisation on cloud condensation nuclei, *Atmos. Environ.*, 42, 5728–5730, 2008. 15229, 15230

Non-linearity in DMS-cloud-climate interactions

M. A. Thomas et al.

Title Page

Abstract

Introduction

Conclusions

References

Tables

Figures

◀

▶

◀

▶

Back

Close

Full Screen / Esc

Printer-friendly Version

Interactive Discussion



Table 1. Percentage mean (DJF mean) change in DIAG1, DIAG2 and DIAG3 for (a) SO₂ column burden (b) H₂SO₄ column burden (c) vertically integrated number of activated particles (Num.act) and (d) aerosol optical depth (AOD) at 0.55 μm averaged over 30° S–75° S.

Diagnostics ↓ // Parameters →	SO ₂	H ₂ SO ₄	Num.act	AOD
DIAG1	118.1	119.0	116.7	23.1
DIAG2	294.5	180.6	179.2	50.3
DIAG3	80.9	28.2	28.9	20.6

Non-linearity in DMS-cloud-climate interactions

M. A. Thomas et al.

Title Page

Abstract

Introduction

Conclusions

References

Tables

Figures

◀

▶

◀

▶

Back

Close

Full Screen / Esc

Printer-friendly Version

Interactive Discussion



Table 2. Percentage mean change in DIAG1, DIAG2, DIAG3 for zonally averaged CDNC burden over 30° S–75° S latitudinal belt.

Diagnostics ↓ // Mon. →	December	January	February	March
DIAG1	103.9	112.9	114.2	83.0
DIAG2	160.3	165.8	169.5	135.1
DIAG3	27.7	24.9	25.8	28.5

Non-linearity in DMS-cloud-climate interactions

M. A. Thomas et al.

Title Page

Abstract

Introduction

Conclusions

References

Tables

Figures

⏪

⏩

◀

▶

Back

Close

Full Screen / Esc

Printer-friendly Version

Interactive Discussion



Table 3. Percentage mean change in DIAG1, DIAG2, DIAG3 for the zonally averaged CD effective radii over 30° S–75° S latitudinal belt.

Diagnostics ↓ // Mon. →	December	January	February	March
DIAG1	−6.32	−5.96	−6.04	−5.36
DIAG2	−9.16	−8.36	−9.03	−7.90
DIAG3	−3.04	−2.56	−3.18	−2.68

Non-linearity in DMS-cloud-climate interactions

M. A. Thomas et al.

Title Page

Abstract

Introduction

Conclusions

References

Tables

Figures

◀

▶

◀

▶

Back

Close

Full Screen / Esc

Printer-friendly Version

Interactive Discussion



Table 4. Percentage mean change in DIAG1, DIAG2, DIAG3 for the zonally and vertically averaged cloud liquid water over 30° S–75° S latitudinal belt.

Diagnostics ↓ // Mon. →	December	January	February	March
DIAG1	39.8	43.8	47.7	42.5
DIAG2	56.8	59.7	65.3	60.1
DIAG3	12.2	11.1	11.9	12.3

Non-linearity in DMS-cloud-climate interactions

M. A. Thomas et al.

Table 5. Top of the atmosphere, all sky radiative forcing in control DMS emission (given in brackets) and double DMS emissions case over the latitudinal belts as given in the table during the SH summer months.

Diagnostics ↓ // Mon. →	December	January	February	March
45° S–30° S	–19.02 (–13.24)	–18.69 (–13.98)	–19.21 (–14.07)	–14.77 (–10.65)
60° S–45° S	–24.83 (–17.67)	–24.85 (–18.57)	–18.33 (–13.86)	–9.90 (–6.98)
75° S–60° S	–9.21 (–7.67)	–9.96 (–7.71)	–6.13 (–5.06)	–2.32 (–1.71)

[Title Page](#)
[Abstract](#)
[Introduction](#)
[Conclusions](#)
[References](#)
[Tables](#)
[Figures](#)
[Back](#)
[Close](#)
[Full Screen / Esc](#)
[Printer-friendly Version](#)
[Interactive Discussion](#)


Non-linearity in DMS-cloud-climate interactions

M. A. Thomas et al.

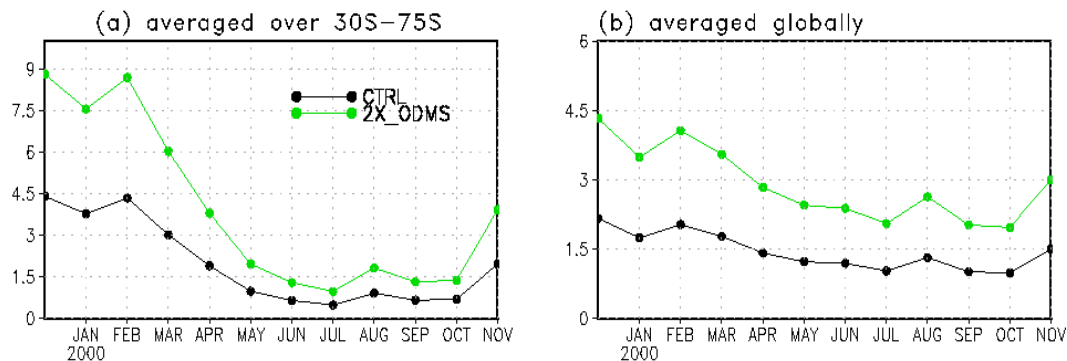


Fig. 1. Time series of ocean DMS emissions in $\text{Kg(S)} \text{m}^{-2} \text{s}^{-1}$ in the 2X_ODMS (open circled line) and CTRL (plain line) simulations **(a)** averaged over $30^\circ \text{S}–75^\circ \text{S}$ and **(b)** averaged globally. The emissions are multiplied by 10^{12} .

[Title Page](#)
[Abstract](#)
[Introduction](#)
[Conclusions](#)
[References](#)
[Tables](#)
[Figures](#)
[◀](#)
[▶](#)
[◀](#)
[▶](#)
[Back](#)
[Close](#)
[Full Screen / Esc](#)
[Printer-friendly Version](#)
[Interactive Discussion](#)


Non-linearity in DMS-cloud-climate interactions

M. A. Thomas et al.

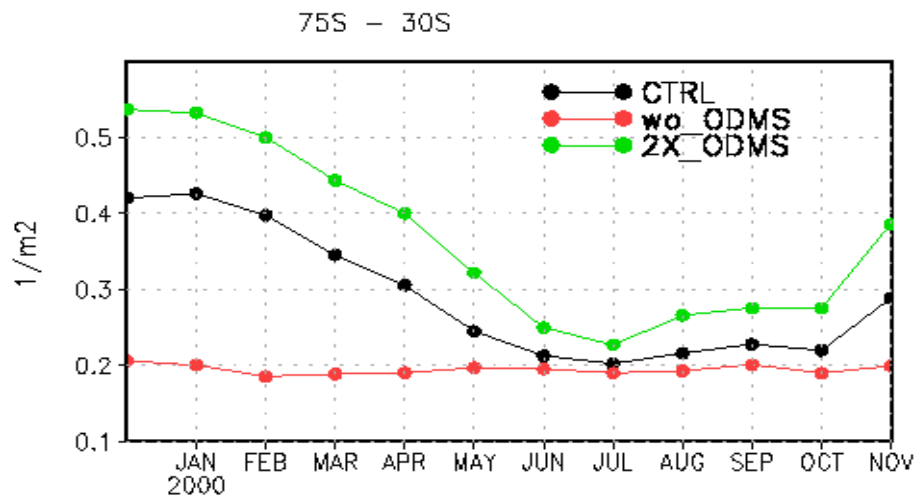


Fig. 2. Latitudinally averaged (30°S – 75°S) time series (December 1999–November 1999) of the vertically integrated CDNC (1 m^{-2}) shown as absolute values in (a) CTRL simulation denoted by the black line (b) wo_ODMS simulation denoted by the red line and (c) 2X_ODMS simulation denoted by the green line. The variables are multiplied by 10^{-11} .

Title Page

Abstract

Introduction

Conclusions

References

Tables

Figures

◀

▶

◀

▶

Back

Close

Full Screen / Esc

Printer-friendly Version

Interactive Discussion



**Non-linearity in
DMS-cloud-climate
interactions**

M. A. Thomas et al.

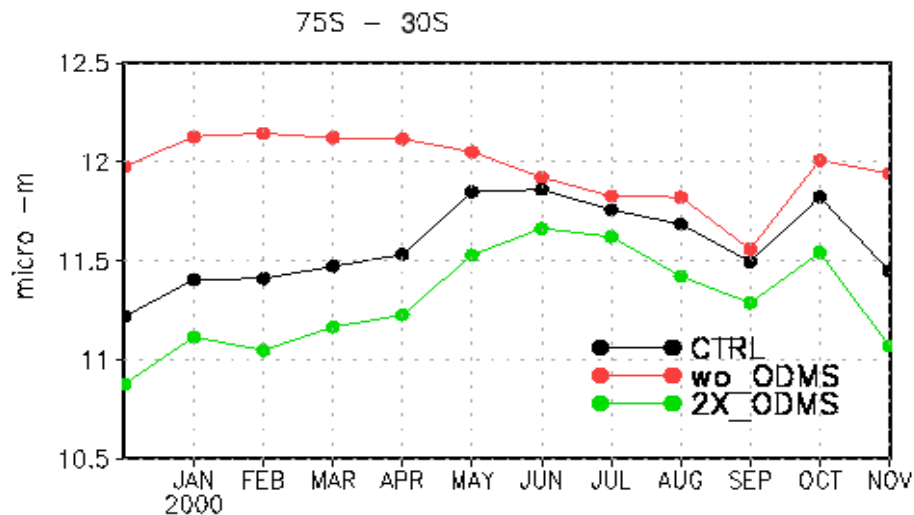


Fig. 3. Same as in Fig. 2, but, for, the cloud droplet effective radii (μm).

[Title Page](#)[Abstract](#)[Introduction](#)[Conclusions](#)[References](#)[Tables](#)[Figures](#)[◀](#)[▶](#)[◀](#)[▶](#)[Back](#)[Close](#)[Full Screen / Esc](#)[Printer-friendly Version](#)[Interactive Discussion](#)

**Non-linearity in
DMS-cloud-climate
interactions**

M. A. Thomas et al.

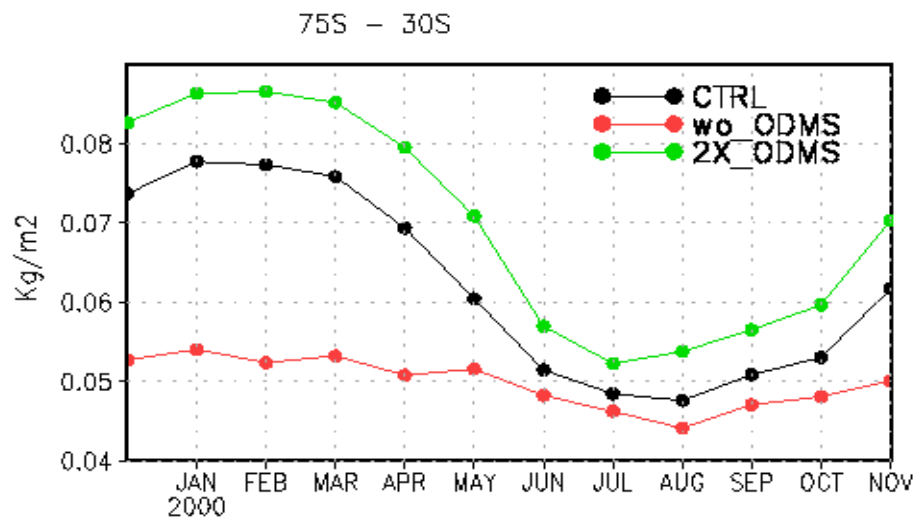


Fig. 4. Same as Fig. 2, but, for, the cloud liquid water path (Kg m^{-2}).

[Title Page](#)[Abstract](#)[Introduction](#)[Conclusions](#)[References](#)[Tables](#)[Figures](#)[◀](#)[▶](#)[◀](#)[▶](#)[Back](#)[Close](#)[Full Screen / Esc](#)[Printer-friendly Version](#)[Interactive Discussion](#)